

# A Way to Stable, Highly Emissive Fluorubine Dyes: Tuning the Electronic Properties of Azaderivatives of Pentacene by Introducing Substituted Pyrazines

Jan Fleischhauer,<sup>\*[a]</sup> Stefan Zahn,<sup>[b]</sup> Rainer Beckert,<sup>\*[c]</sup> Ulrich-Walter Grummt,<sup>[d]</sup> Eckhard Birckner,<sup>[d]</sup> and Helmar Görls<sup>[e]</sup>

*One life ends another begins—In memoriam to Nelly Jahn 18.07.1997–29.09.2011—You will be forever in our hearts*

**Abstract:** Pentacene and its derivatives are among the most important examples of  $\pi$ -electron-rich molecules used in organic field effect transistors. The replacement of CH groups by nitrogen atoms opens an elegant way to generate highly electron-deficient molecules, known as oligoazaacenes. We describe the synthesis and spectroscopic properties of two novel derivatives of this family, namely the zwitterionic and quinoidal conjugated forms of dihydro-5,6,7,12,13,14-hexaazapentacene (fluorubine). We outline a powerful strategy

to tune the electronic properties of these redox-active azaacenes by the selective introduction of substituted pyrazines. Their acidochromic and solvatochromic behaviour is investigated experimentally and interpreted with the help of theoretical calculations. The simple “exchange” of substituents or

**Keywords:** azo compounds • density functional calculations • dyes/pigments • heterocycles • hexaazapentacenes

protonation is shown to significantly alter the spectroscopic and electronic properties of these remarkably stable  $\pi$ -systems. Their exceptional optical properties, such as high fluorescence quantum yields combined with a redox-active behaviour, make them promising candidates for sensor materials. Additional marked features in the solid state, such as herringbone packing in combination with short  $\pi$ - $\pi$  distances, will open access to electronic materials.

## Introduction

The field of molecular organic materials has gained significant importance in recent decades. Organic materials have been successfully applied as the active components in photovoltaic devices, molecular diagnostics, photodynamic therapy (PDT), optical data storage, organic light-emitting diodes (OLEDs) and organic field effect transistors (OFETs).<sup>[1]</sup> Pentacene and its derivatives have been established as benchmark  $\pi$ -electron-rich materials, and are particularly important in OFETs as they display high hole mobility in the solid state.<sup>[1a,2]</sup> Nitrogen substitution in the pentacene scaffold has been proposed as a potentially fruitful route to build up n-type molecules, and so oligoazaacenes have become the subject of increased interest in theoretical chemistry and material science.<sup>[2,3]</sup> More recently, excellent reviews have been published covering historical aspects and modern developments of azaacenes.<sup>[2]</sup> Here, we demonstrate how the molecular properties of compounds **1–5** can be tuned by altering their nitrogen substitution pattern by fixing the different hydroforms by non-hydrogen substituents, and further refining by protonation or alkylation.

It has been proven that the replacement of two CH groups with nitrogen atoms gives p-type materials, such as 5,14-dihydrodiazapentacene (5,14-DDP)<sup>[4a]</sup>, whereas higher substitution levels can give rise up to n-type conductors, as exemplified by 5,7,12,14-tetraaza-6,13-pentacenequinone

[a] Dr. J. Fleischhauer  
Ruprecht-Karls-University Heidelberg  
Department of Chemistry  
Im Neuenheimer Feld 270  
69120 Heidelberg (Germany)  
Fax: (+49) 6221-548404  
E-mail: j.fleischhauer@oci.uni-heidelberg.de

[b] Dr. S. Zahn  
Monash University, School of Chemistry  
Clayton, Victoria 3800 (Australia)

[c] Prof. Dr. R. Beckert  
Friedrich Schiller-University Jena  
Department of Organic and Macromolecular Chemistry  
Humboldtstr. 10, 07743 Jena (Germany)  
E-mail: Rainer.Beckert@uni-jena.de

[d] Prof. Dr. U.-W. Grummt, Dr. E. Birckner  
Friedrich Schiller-University Jena  
Department of Physical Chemistry  
Lessingstr. 10, 07743 Jena (Germany)

[e] Dr. H. Görls  
Friedrich Schiller-University Jena  
Department of Inorganic Chemistry  
Lessingstr. 8, 07743 Jena (Germany)

 Supporting information for this article (details of synthetic procedures, DFT calculations including Cartesian coordinates of the calculated structures, X-ray structural analysis, CV and UV/VIS measurements) is available on the WWW under <http://dx.doi.org/10.1002/chem.201103350>.



of  $\text{PCl}_5/\text{POCl}_3$  allowed the formation and isolation of tetrachloropyrazine (**7**).<sup>[7b]</sup>

In order to assist chlorine displacement, collidine was found to act as both a high-boiling-point solvent and non-nucleophilic base. Initially, the 1:1 condensation product, 2,3-dichloro-5-phenyl-5,10-dihydropyrazino[2,3-*b*]quinoxaline (**9**), was observed as the main product when the reaction was maintained at 120–130 °C for 2–3 days; and could be isolated in up to 50% yield through precipitation by using dichloromethane/ethanol. Subsequent investigation has shown that intermediates **7** and **9** can act as building blocks for the syntheses of azaacenes **3a** and **4a**. Increasing the reaction temperature and extending the reaction time (140 °C, 5 days) with compound **7**, allowed us to isolate the thermodynamically preferred isomer **4a** as the main product (20%). Unfortunately, the mesoionic derivative **3a** was only isolable in traces (3%). The yields of both isolated compounds are relatively low, which seems to be a more general drawback of this type of condensation reactions. Bunz et al. have investigated the use of Hartwig–Buchwald protocols to generate tetraazapentacenes in high yields.<sup>[8]</sup> An extension of this chemistry may provide an attractive alternative to the condensation reactions presented here. First attempts to apply this strategy to systems of type **7** were not successful and modified cyclisation procedures are currently being investigated in our laboratories.

The poor solubility of model compounds **3a** and **4a** hinders their purification and spectroscopic characterisation.<sup>[9]</sup> In spite of this, we confirmed the structures of **3a** and **4a** by means of MS, HRMS and NMR measurements, and single X-ray analysis of suitable crystals (see the Supporting Information). From chloroform/methanol mixtures we were able to obtain crystals of sufficient quality and confirmed the molecular structures of compounds **3a** and **4a** in the form of their chloroform adducts (Figures 1 and 2). In case of **3a** the phenyl substituents are nearly perpendicular to the slightly twisted hexaazapentacene plane (the torsion angle is  $\approx 3.8^\circ$ ) and in excellent agreement with the results of DFT structure optimisations (level of theory TZVP/PBE(RI); see also Computational Details in the Supporting Information). Due to strong  $\pi$ -interactions, the mesoionic derivative **3a** forms face-to-face stacked dimers ( $d \approx 3.387 \text{ \AA}$ ), which themselves build highly symmetric molecular arrangements in the solid state (Figure 1).

Shortening of the bond lengths C7–N2 (1.326(3) Å), C8–N4 (1.323(2) Å), C16–N6 (1.327(3) Å) as well as C15–N6 (1.330(2) Å) points to partial charge localisation at the central pyrazine core (Figure 1). On the other hand, compound **4a**, though calculations predict it to be 31.3 kJ mol<sup>-1</sup> more stable than compound **3a**, clearly shows the quinoidal structure by a shortening of the C7–N2 (1.310(5) Å) and C8–N3a (1.308(4) Å) bonds and a slight elongation of the C7–N3 (1.371(5) Å) and C8–N1 (1.372(4) Å) bonds, which is also in excellent agreement with the calculated bond parameters of the azaacene framework (Figure 2). contrast to **3a** the scaffold of **4a** is completely planar, whereby the phenyl substituents are twisted out of the azaacene plane by 71°.

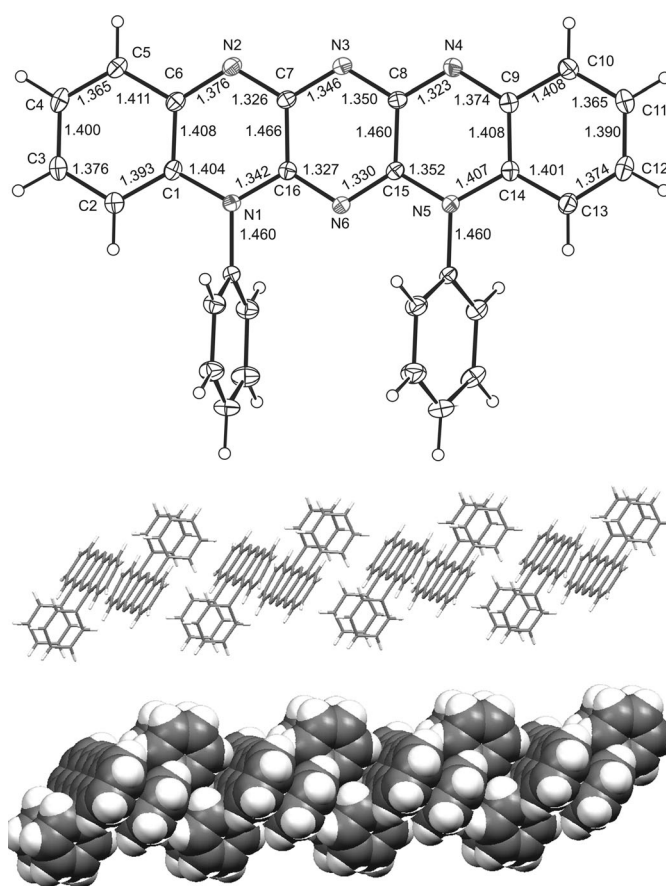


Figure 1. ORTEP plot of the molecular structure (top) and the solid-state packing (bottom) of the mesoionic fluorubine **3a** (50% probability ellipsoids).<sup>[10]</sup> The co-crystallised chloroform molecules are omitted for clarity.

The solid-state derivative **4a**, which co-crystallises with two molecules of chloroform, adopts a herringbone structure in one dimension and a columnar face-to-face packing in the second dimension—similar to rubrene—which is one of the prerequisites for efficient multidimensional charge transport.<sup>[11]</sup> Thereby, the molecular distances are approximately 2.78 Å for the edge-to-face separation and approximately 3.359 Å between molecules that were stacked in parallel (Figure 2). The  $\pi$ – $\pi$ -stacking distances in dimers of **3a** are slightly larger than those obtained by Ariga et al. for aza-pentacene derivative **5** ( $d \approx 3.197 \text{ \AA}$ ),<sup>[5b]</sup> but comparable to those of TAPQ ( $d \approx 3.32 \text{ \AA}$ ).<sup>[4b]</sup>

**Spectroscopic and electronic properties:** In this section, we will illustrate the influence of different pathways of conjugation of the azaacene scaffold on the spectroscopic and electronic properties. Hexaazapentacenes **3a** and **4a** exhibit remarkable spectroscopic properties, which are significantly influenced by the position of the phenyl substituents. Because the electronic structure of the fluorubinium ion **2a** (R = Ph, R' = Me, X = BF<sub>4</sub><sup>-</sup>, Scheme 1)<sup>[5]</sup> resembles the formally methylated derivative of **3a**, we use it as benchmark. The photophysical properties of compounds **2a–4a** are sum-

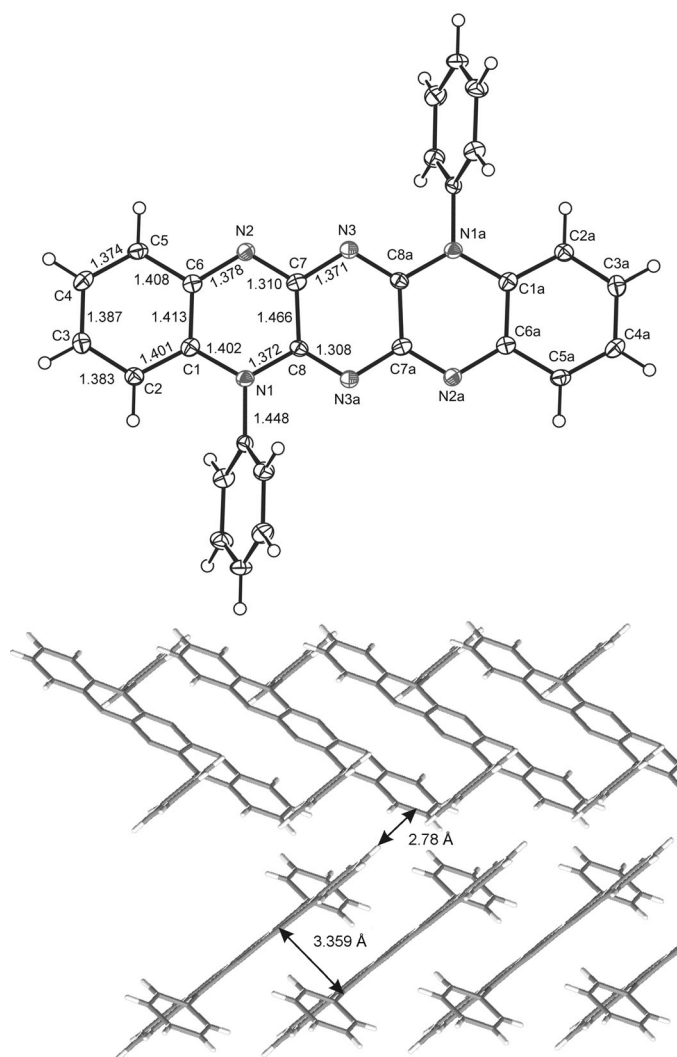


Figure 2. ORTEP plot of the solid-state structure (top) and the solid-state packing (bottom) of the quinoidal fluorubine **4a** (50% probability ellipsoids).<sup>[10]</sup> The co-crystallised chloroform molecules are omitted for clarity.

Table 1. Photophysical data of selected hexaazapentacenes in DCM, 36% HCl and acetic acid.

	Solvent	$\lambda_{\max}^{\text{abs}}$ [nm]	$\lambda_{\max}^{\text{em}}$ [nm]	$\Delta\nu_{\text{St}}^{\text{[a]}}$ [ $\text{cm}^{-1}$ ]	$\phi_{\text{f}}^{\text{[b]}}$	$\tau^{\text{[c]}}$ [ns]	$k_{\text{f}}^{\text{[c]}}$ [ $\text{ns}^{-1}$ ]	$k_{\text{nr}}^{\text{[c]}}$ [ $\text{ns}^{-1}$ ]	$\epsilon^{\text{[a]}}$ [ $\text{M}^{-1}\text{cm}^{-1}$ ]
<b>2a</b>	$\text{CH}_2\text{Cl}_2$	535	546	380	0.95	4.32	0.22	0.012	80 000
	AcOH	525	543	630	0.95	4.47	0.21	0.011	67 700
<b>2Ha</b>	HCl (36%)	540	557	570	0.17	1.0	0.17	0.83	n.d. <sup>[d]</sup>
<b>3a</b>	$\text{CH}_2\text{Cl}_2$	609	642	840	0.58	7.20	0.081	0.058	48 600
<b>3Ha</b>	AcOH	525	577	1720	0.72	4.14	0.17	0.068	67 700
<b>3HHa</b>	HCl (36%)	583	596	370	0.31	2.16	0.14	0.32	n.d.
<b>4a</b>	$\text{CH}_2\text{Cl}_2$	513	516	110	1	3.27	0.31	<0.004	98 800
<b>4Ha</b>	AcOH	548	569	670	0.66	3.94	0.17	0.086	57 400
<b>4HHa</b>	HCl (36%)	582	595	380	0.24	1.70	0.14	0.45	n.d.

[a] Determined for the longest wavelength transition. [b] The fluorescence quantum yields  $\phi_{\text{f}}$  (error  $\pm 10\%$ ) were calculated according to the literature relative to rhodamine 6G in ethanol used as a standard ( $\phi_{\text{f}}=95\%$ ).<sup>[13]</sup> The absorbance at the excitation wavelength was kept below 0.05 for the samples and the standard. [c] Details for photophysical determination of fluorescence life times ( $\tau$ ), rates of radiative decay ( $k_{\text{f}}$ ) and rates of non-radiative decay ( $k_{\text{nr}}$ ) are listed in the Supporting Information. [d] Not determined.

marised in Table 1. In dichloromethane, the purple solution of the zwitterionic derivative **3a** exhibits a broad structured  $\pi \rightarrow \pi^*$  transition between  $\lambda = 500$  and 610 nm with moderate to high extinction coefficients, where the vibronic coupling can be related to an in-plane skeletal mode of the aromatic ring system (Figure 3 top,  $\tilde{\nu} \approx 1320 \text{ cm}^{-1}$ ). Typical for zwitterionic compounds, compound **3a** shows a pronounced negative solvatochromic behaviour (see the Supporting Information). The peak absorption ( $\lambda_{\max}^{\text{abs}}$ ) of compound **3a** shifts hypsochromically from  $\lambda = 630$  to 588 nm by going from toluene to methanol. By comparing to previous structure-property-relationship elucidations of related mesoionic 5,7,12,14-tetraazapentacenes, these spectra are hypsochromically shifted about 160 nm, which is remarkable.<sup>[11a]</sup> As indicated by the solvent-dependent Stokes shift ( $\Delta\nu_{\text{St}}$ ), and further supported by DFT calculations (def-SV(P)/BP86), the chromophore **3a** exhibits a small change in its dipole moment ( $\mu$ ) going from its ground (7.90 D) to first excited state (5.80 D). Decreasing the dipole moment during excitation results in an Franck-Condon excited state that is formed in a more strained surrounding solvent cage of oriented dipole molecules. Thus increased solvent polarity energetically stabilises the ground state more than the excited state and leads to pronounced hypsochromically shifted absorption spectra.<sup>[12]</sup> In case of the fluorubinium ion **2a** a less-pronounced negative solvatochromic behaviour combined with small Stokes shifts was observed,<sup>[5]</sup> which can be attributed to a decreased change of its dipole moment by going from the ground to the first excited state.

As described here, the apparently simple “exchange” of a phenyl substituent from position 7 to 12 significantly alters the optical properties of the hexaazapentacenes **3a** and **4a**. The yellow solution of the quinoidal derivative **4a** exhibits a well-structured  $\pi \rightarrow \pi^*$  transition between  $\lambda = 400$  and 520 nm showing vibronic couplings (Figure 3 bottom,  $\tilde{\nu} \approx 1390 \text{ cm}^{-1}$ ) and high extinction coefficients. In contrast to compounds **2a** and **3a**, the UV/VIS absorption of **4a** shows no solvatochromic behaviour as the dipole moments of the ground and excited state of **4a** are almost identical, resulting in a negligible Stokes shift of  $110 \text{ cm}^{-1}$ . Within experimental error, in  $\text{CH}_2\text{Cl}_2$  compound **4a** exhibits a very high fluorescence quantum yield ( $\phi_{\text{f}}$ ), which is comparable with Rhodamine 6G and the hexaazapentaceniium salt **2a**.<sup>[5]</sup> The mesoionic dye **3a** exhibits a slightly smaller  $\phi_{\text{f}}$  of 0.58 that is orders of magnitude higher than that of related derivatives.<sup>[11a]</sup>

The UV/VIS spectra acquired in glacial acetic acid differ significantly from those obtained in  $\text{CH}_2\text{Cl}_2$ , whereby the absorption of **3a** is blue-shifted by 84 nm. Furthermore, the absorption and emission transitions are more structured and have increased extinction coefficients ( $\epsilon$ ) as well as  $\phi_{\text{f}}$  values. The observed longest wavelength transition does not match the expected relationship to the solvent polarity, but the spectroscopic behaviour is similar to that of **2a**, pointing to a monoprotonated

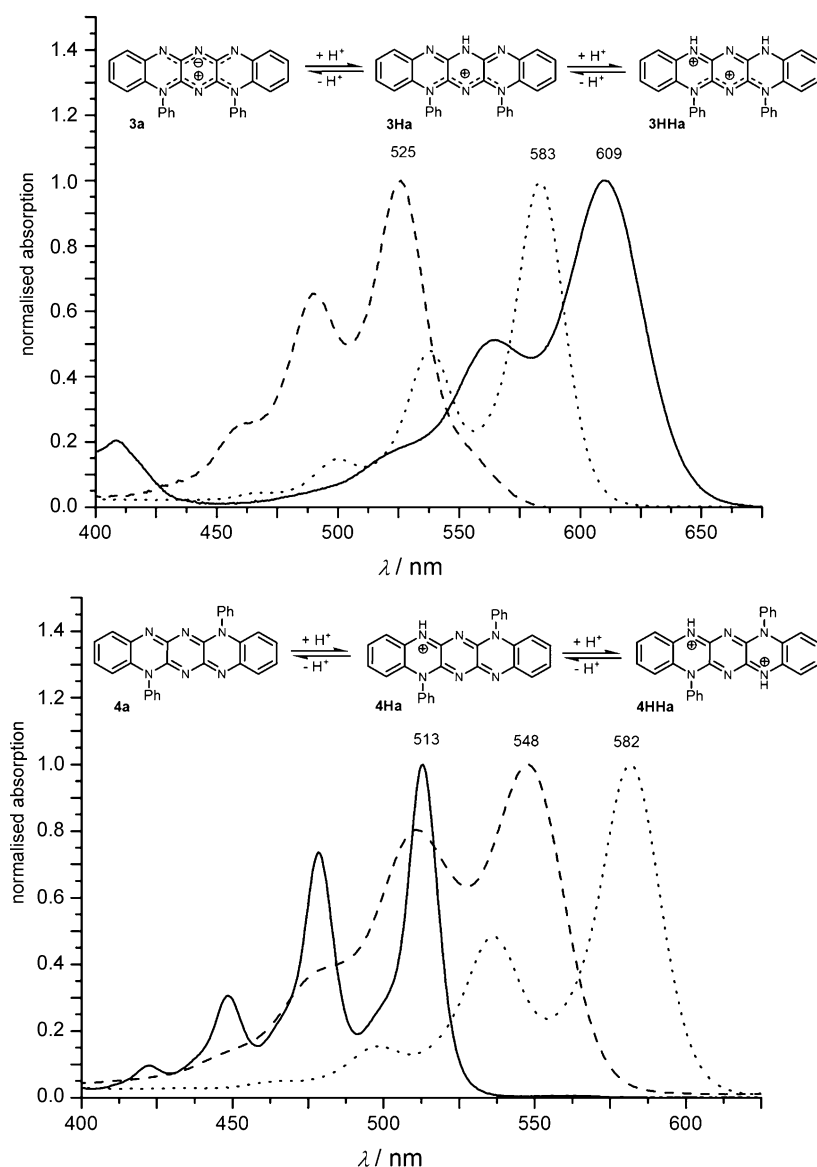


Figure 3. Normalised absorption spectra of the longest wavelength transitions of the neutral (left), mono (middle) and double-protonated (right) fluorubines **3a** (top) and **4a** (bottom) in their most stable tautomeric forms as indicated by DFT calculations (TZVP/PBE(RI); — =  $\text{CH}_2\text{Cl}_2$ , - - - = AcOH, ····· = HCl (36 %)).

species, such as those of **3Ha**. This species was calculated to be the most favoured single-protonated species (Figure 3). It is worth noting this structural similarity, because **2a** represents the formal alkylation product of **3a**. By going from dichloromethane to acetic acid the absorption and emission spectra of benchmark **2a**, which is not protonated under these conditions, are shifted hypsochromically and in agreement with previously observed negative solvatochromism of azaaceniuniumsalts of type **2**.<sup>[5]</sup> In comparison to **2a**, the decreased fluorescence quantum yield of **3a** can be attributed to the protonated nitrogen atom that may open non-radiative deactivation pathways. In hydrochloric acid, that is under more acidic conditions, a more structured absorption spectrum of compound **3a** was observed, bathochromically shifted compared to AcOH (Ac = acyl) though blue-shifted

relative to  $\text{CH}_2\text{Cl}_2$ , which indicates the presence of the double-protonated species **3HHa**. The relative quantum yield  $\phi_f$  of the species is further decreased to 31%. In hydrochloric acid the positively charged hexaazapentaceniun ion **2a** will be additionally protonated to furnish **2Ha**. This protonated derivative represents a formally mixed analogue to **3HHb**, but is energetically less preferred as compared to **3HHa** (for details see the Supporting Information). In contrast to **3a**, monoproteination of compound **4a** in aqueous acetic acid leads to a broadened and bathochromically shifted absorption spectrum combined with lower  $\epsilon$  and  $\phi_f$  values. Double protonation of **3a** and **4a** in hydrochloric acid is supported by increased solubility in aqueous media, and a shift in colour to dark purple. In case of the double-protonated azaaceniunium ions **3HHa** and **4HHa** the UV/VIS spectra are almost superimposable and show a structured absorption at approximately 582 nm (Figure 3). For both isomers, this observation can be explained by one of Döhnes colour rules, which states that non-alternating polymethines exhibit particularly bathochromic absorption.<sup>[14]</sup> Obviously, successive protonation of **3a** and **4a** leads to non-alternating polymethine chromo-

phores. The fluorescence life times ( $\tau$ ) of compounds **2a–4a** typically ranges from 2 to 4 ns, whereby we observed a mono-exponential decay and good correlation between the rates of radiative deactivation ( $k_f$ ) and the Strickler–Berg equation (see the Supporting Information). In all investigated solvents, the values of the radiative decay of compounds **2a–4a** are in the same range, within the experimental error. On the other hand  $\tau$  and  $\phi_f$  decreases significantly by going from  $\text{CH}_2\text{Cl}_2$  or acetic acid to hydrochloric acid, whereby the rates of non-radiative decay ( $k_{nr}$ ) increase by a factor of five, pointing to a strong solvent effect in case of hydrochloric acid.

Gas-phase DFT calculations were initially completed for all the competing neutral and protonated species, with the substituents labelled R in Scheme 1 fixed as hydrogen, by

using the Gaussian 03<sup>[15]</sup> program on the theoretical levels of 6-31+G/B3LYP and 6-31+G\*/B3LYP. Starting from these optimised structures the longest wavelength transitions were estimated (see the Supporting Information). Because hydrogen substitution offers only a simplified means to compare the different hydroforms, the phenyl-substituted derivatives were additionally modelled. The calculated longest wavelength transitions ( $\lambda_{\text{max}}^{\text{abs}}$ ) and oscillator strengths ( $f$ ) of **3a** and **4a** (and of their hypothetical reference structures, in which the aromatic substituents have been replaced by hydrogen) are in acceptable agreement to the experimental results and are listed in the Supporting Information. The photophysical properties of compounds **3a** and **4a**, particularly their high extinction coefficients and fluorescence quantum yields, make these scaffolds ideal for designing new chromophores for chemical biology or molecular diagnostics. In case of **3a** these properties go hand in hand with a pronounced solvatochromic behaviour, making it a strong candidate for novel multi-parameter chromophores, which are used to probe and correlate different parameters at the same time, for example, location of participation and polarity of the surrounding microenvironment or cell dynamics.<sup>[16]</sup>

**Prototropism:** As can be observed from the photophysical data, the electronic properties of the dihydrohexaazapentacenes are strongly dependent on the substitution pattern of the central pyrazine core. This impressive feature is limited to non-hydrogen substituents at the attended pyrazine moieties, leading to the fixing of benzoid (**1**), quinoidal (**4**) and zwitterionic (**3**) structures. As a result of gas-phase calculations with the TURBOMOLE<sup>[17]</sup> program suite employing the TZVP/PBE(RI) method, it was found that in comparison to **3a** that was used as reference system (0 kJ mol<sup>-1</sup>), the benzoid conjugated derivative **1a** (R=Ph, -63.1 kJ mol<sup>-1</sup>) is energetically preferred followed by compounds **4a** (-31.1 kJ mol<sup>-1</sup>) and **5a** (-29.4 kJ mol<sup>-1</sup>). It is worthy to note, that up to now there are only few simplified theoretical studies that consider the influence of this range of conjugation pathways on the electronic properties of related hexaazaacene systems.<sup>[51–53]</sup> The various possible mono- and double-protonated regioisomers of compounds **3a** and **4a** were subsequently investigated, and the energetically most favoured forms (**3Ha**, **4Ha**, **3HHa**, **4HHa**) are included in Figure 3.

In case of derivative **3a** the first protonation at the central pyrazine moiety (C ring Scheme 1 and Figure 3) is energetically preferred, whereas the peripheral pyrazine moiety (B ring) is the favoured initial protonation site of the quinoidal hexaazapentacene **4a**. In the case of **3Ha** the optimised

structure is almost identical to those of the cationic fluorobine derivative **2a**, which explains their similar spectroscopic behaviour. However, the energy differences between each set of single-fold protonated isomers of **3a** and **4a** are relatively small, so it is assumed that both compounds exist in a dynamic equilibrium within their different protonated forms (see the Supporting Information). The models also indicate that double protonation of **3a** and **4a** occurs predominantly at the peripheral pyrazine rings (B and D ring), which may account for the similar optical properties of **3HHa** and **4HHa**.

The improved solubility mediated by protonation or alkylation is further evidence for the presence of strong  $\pi$ - $\pi$ -interactions, because introduction of charged nitrogen atoms leads to increased repulsion forces between the molecules. As mentioned above, with strong acids the hexaazapentacenes **3a** and **4a** were protonated twice, resulting in water solubility as well as changes to the optical properties. These protonations are reversible, so that addition of base regenerates **3a** and **4a**. In case of azaacene **4a** we were able to obtain single crystals from hydrochloric acid, suitable for X-ray structural analysis, which supports the results obtained by DFT calculations (see the Supporting Information). Even in the protonated state, the hexaazapentacene plane of **4HHa** tends to form dimers through  $\pi$ - $\pi$  interactions. It is clearly observable that the quinoidal substructure is still preserved, with the double bond lengths of C7–N2 (1.321(2) Å) and C8–N3a (1.323(2) Å), being slightly elongated compared to their equivalents in the uncharged derivative **4a**.

**Electronic properties:** Detailed structural analysis by using the DFT approach on the level of TZVP/PBE(RI) offered insights into the chromophore and particularly its charge delocalisation and aromaticity (see Computational Details in the Supporting Information). Figure 4 depicts the electro-

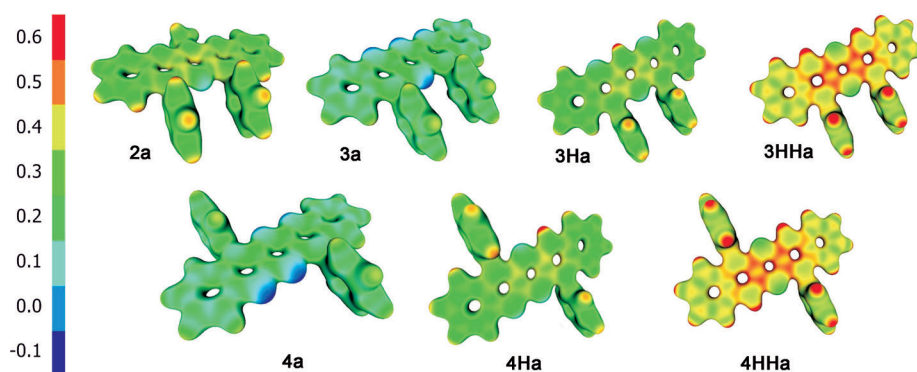


Figure 4. Electrostatic potentials of azaacenes **2a–4a** as well as their mono- and double-protonated counterparts at the isodensity surface with 0.05e/bohr<sup>3</sup> (TZVP/PBE(RI))

static potential surfaces of the most important compounds. In general, the non-substituted nitrogen atoms carry the majority of the electron density, whereas the positive charge is localised at the hydrogen atoms. Successive protonation of the azaacene core leads to increased charge at the carbon

atoms of the central pyrazine ring. From there, it spreads to the two other pyrazine moieties and finally to the annulated benzene moieties. The Hirschfeld partial charge analysis<sup>[18]</sup> underlines this finding and shows the similarity between **3Ha** and **2a**. An additional Wiberg bond order analysis<sup>[19]</sup> and calculation of the nucleus-independent chemical shifts (NICS)<sup>[20]</sup> by using benzene and pyrazine as references, confirmed that the pyrazine nitrogen substituents significantly influence the electronic conjugation of the azaacenes. The NICS values of the peripheral benzene moieties are similar to the reference system and approach benzene when protonated. Additionally, the NICS values of the benzene moieties of the benzoid conjugated derivatives **1a** and **5a** (R = Ph, A and E rings) are more benzene-like than those of **3a** and **4a**. It should be noted that the NICS values of the aryl-substituted pyrazine moieties differ significantly from those of their unfunctionalised annulated analogues and the ideal theoretical value of pyrazine itself. The same trend was observed by inspection of the deviations of Wiberg bond order analysis for which the aryl-functionalised rings show the strongest discrepancies to the aromatic reference as well.

The corresponding frontier orbitals are fully delocalised over the whole molecule. By inspecting the values of the HOMO/LUMO orbitals it becomes clear that selective functionalisation of the pyrazine core, that is, by altering the peripheral substituents or by subsequent protonation or alkylation, represents a powerful tool to tune the electronic properties of the hexaazapentacenes presented here. In this study, auxochromic groups such as alkoxy substituents have not been included. Such groups will alter the absorption and emission wavelengths and give rise access to large regions of the UV and visible spectrum.

In case of **3a** and **4a** the calculated energy levels of the LUMO orbitals match very well to those obtained by cyclic voltammetric (CV) measurements, although the energies of the HOMO orbitals were systematically overestimated (see the Supporting Information). Unfortunately, in case of the charged derivatives (i.e., **2a**, **3Ha**, **3HHa**, **4Ha** and **4HHa**) the calculated values of the frontier orbitals are less satisfying and can be only regarded as rough estimation. Not that surprisingly, it was also observed that the values of the corresponding orbitals strongly depend on the applied level of theory. More accurate HOMO energy levels should be available by using Hartree–Fock (HF) calculations for which the RIJ-COSX approximation was employed (see the Computational Details in the Supporting Information), but no significant improvement was observed for our systems. Because the malfunction of DFT for orbital energies is well known<sup>[21]</sup> and solvation might also influence the orbital energy, we use these calculations only to illustrate trends. There already exist refined approaches such as AIMD calculations that consider aspects such as solvation, but here we are limited due to computational capacities. It is worth noting, that the measured LUMO energy levels (electron affinities) of **3a** and **4a** already reach the required values ( $\approx 3$  eV) to allow efficient electron injection from metal electrodes, making these materials strong candidates for n-type OFET devi-

ces.<sup>[3b]</sup> On the other hand, the band-gap energies measured by CV are in excellent agreement to those obtained by optical methods. Figure 5 summarises the results of DFT investigations and is illustrating how in principle the energies of frontier orbitals can be modified by the factors discussed above.

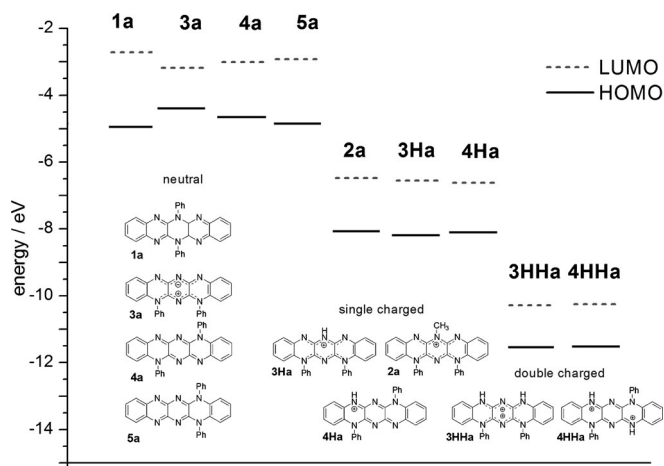


Figure 5. Calculated energy of the frontier orbitals of neutral and charged azaacenes **1a–5a**, showing the dependence of the energies on the substitution of the chromophore core (method: TZVP/PBE(RI)).

These chromophores can be considered as formal anti-aromatic and stable 24  $\pi$ -electron systems. The reduced (**3a** × RED/**4a** × RED, 26  $\pi$  electrons) and oxidised (**3a** × OX/**4a** × OX, 22  $\pi$  electrons) species represent formal  $4n+2$  aromatic systems, though they are energetically disfavoured compared to their formal  $4n$  anti-aromatic counterparts **3a** and **4a**. These findings are in agreement to those of related systems, where it was found that the formal anti-aromatic oligoazaacenes become energetically more favourable by expanding the  $\pi$ -system.<sup>[2d,3e]</sup> We wish to note that clear evidence for the leuco-dye form of compounds **3a** and **4a** is observable, by both CV measurements and through chemical reduction. Reducing the systems in aqueous THF solutions with sodium dithionite leads to hypsochromically shifted absorption and emission bands of the leuco-dye forms (**3a** × RED  $\lambda_{\text{max}} = 466$ ,  $\lambda_{\text{em}} = 546$  nm), which are quickly re-oxidised when exposed to air. Hexaazapentacenes **3a** and **4a** also exhibit complex cyclic voltammograms with two irreversible oxidation peaks and two quasi-reversible reduction peaks (CV in  $\text{CH}_2\text{Cl}_2$  on glassy carbon as counter and working electrode and with glassy carbon//Ag/AgCl as the reference electrode; see the Supporting Information) and similar complex CV spectra have been previously observed for other dihydroderivatives of azaacenes.<sup>[5h]</sup> More detailed studies of redox activity are beyond the scope of this paper, because different prototropic and hydroforms may contribute in a complex way<sup>[5h,j]</sup> and will be described in subsequent work.

## Conclusion

We introduced tetrachloropyrazine as a building block for the synthesis of oligoazaacenes and obtained two novel fluoro-rubine derivatives. These regioisomeric derivatives were characterised by NMR spectroscopy, MS, X-ray structural analysis and UV/VIS measurements as well as DFT methods. Strong packing effects were observed in the solid structure due to marked  $\pi$ - $\pi$ -interactions, which were proven by X-ray structural analysis and ab-initio calculations of model compounds **3a** and **4a**. We discussed their exceptional optical properties, such as their high fluorescence quantum yields, which are comparable to those of rhodamine 6G, as well as their strong solvatochromic and acidochromic behaviour. We have demonstrated the tuning of the electronic properties of azaacenes by selective introduction of substituted pyrazines. These chromophores are promising candidates for functional materials, and particularly for electro-optical devices, because of their pronounced  $\pi$ -interactions and redox activity. In forthcoming publications we will detail improved synthetic procedures that allow us to introduce functionalities in a selective manner, and we will report on their ability to act as n-type conducting materials for OFET devices.

## Acknowledgements

We would like to thank E. Kielmann for measuring photophysical data, DFG for founding of postdoctoral fellowship (FL720/1-1), and H. A. Collins and J. K. Sprafke for language polishing.

- [1] a) S. Sun, L. R. Dalton in *Introduction to Organic Electronic and Optoelectronic Materials and Devices*, CRC, London, **2008**; b) A. Pron, P. Gawrys, M. Zagorska, D. Djurado, R. Demadrille, *Chem. Soc. Rev.* **2010**, *39*, 2577–2632; c) Y.-J. Cheng, S.-H. Yang, C.-S. Hsu, *Chem. Rev.* **2009**, *109*, 5868–5923; d) J. P. Celli, B. Q. Spring, I. Rizvi, C. L. Evans, K. S. Samkoe, S. Verma, B. W. Pogue, T. Hasan, *Chem. Rev.* **2010**, *110*, 2795–2838; e) A. Hagfeldt, G. Boschloo, L. Sun, L. Kloo, H. Pettersson, *Chem. Rev.* **2010**, *110*, 6595–6663; f) K. Szacilowski, W. Macyk, A. Drzewiecka-Matuszek, M. Brindell, G. Stochel, *Chem. Rev.* **2005**, *105*, 2647–2694; g) A. Mishra, C.-Q. Ma, P. Bäuerle, *Chem. Rev.* **2009**, *109*, 1141–1276; h) A. R. Murphy, J. M. J. Fréchet, *Chem. Rev.* **2007**, *107*, 1066–1096; i) A. W. Hains, Z. Liang, M. A. Woodhouse, B. A. Gregg, *Chem. Rev.* **2010**, *110*, 6689–6735; j) A. Mishra, R. K. Behera, P. K. Behera, B. K. Mishra, G. B. Behera, *Chem. Rev.* **2000**, *100*, 1973–2011; k) Y. Shiota, H. Kageyama, *Chem. Rev.* **2007**, *107*, 953–1010; l) W. Wu, Y. Liu, D. Zhu, *Chem. Soc. Rev.* **2010**, *39*, 1489–1502.
- [2] a) M. Bendikov, F. Wudl, D. F. Perepichka, *Chem. Rev.* **2004**, *104*, 4891–4945; b) J. E. Anthony, *Chem. Rev.* **2006**, *106*, 5028–5048; c) J. E. Anthony, A. Facchetti, M. Heeney, S. R. Marder, X. Zhan, *Adv. Mater.* **2010**, *22*, 3876–3892; d) U. H. F. Bunz, *Chem. Eur. J.* **2009**, *15*, 6780–6789; e) U. H. F. Bunz, *Pure Appl. Chem.* **2010**, *82*, 953–968; f) G. J. Richards, J. P. Hill, T. Mori, K. Ariga, *Org. Biomol. Chem.* **2011**, *9*, 5005–5017.
- [3] a) C. P. Constantinides, P. A. Koutentis, J. Schatz, *J. Am. Chem. Soc.* **2004**, *126*, 16232–16241; b) M. Winkler, K. N. Houk, *J. Am. Chem. Soc.* **2007**, *129*, 1805–1815; c) S. Miao, S. M. Brombosz, P. von R. Schleyer, J. I. Wu, S. Barlow, S. R. Marder, K. I. Hardcastle, U. H. F. Bunz, *J. Am. Chem. Soc.* **2008**, *130*, 7339–7344; d) J. E. Anthony, *Angew. Chem.* **2008**, *120*, 460–492; *Angew. Chem. Int. Ed.* **2008**, *47*, 452–483; e) J. I. Wu, C. S. Wannere, Y. Mo, P. von R. Schleyer, U. H. F. Bunz, *J. Org. Chem.* **2009**, *74*, 4343–4349; f) R. Scipioni, M. Boero, G. J. Richards, J. P. Hill, T. Ohno, T. Mori, K. Ariga, *J. Chem. Theory Comput.* **2010**, *6*, 517–525; g) R. Scipioni, J. P. Hill, F. J. Richards, M. Boero, T. Mori, K. Ariga, T. Ohno, *Phys. Chem. Chem. Phys.* **2011**, *13*, 2145–2150.
- [4] a) Q. Miao, T.-Q. Nguyen, T. Someya, G. B. Blanchet, C. Nuckolls, *J. Am. Chem. Soc.* **2003**, *125*, 10284–10287; b) Q. Tang, Z. Liang, J. Liu, J. Xu, Q. Miao, *Chem. Commun.* **2010**, *46*, 2977–2979.
- [5] a) O. Hinsberg, E. Schwantes, *Chem. Ber.* **1903**, *36*, 4039–4050; b) J. L. Switzer, US Patent 2.495.202, **1945**; c) F. Graser, DE3504143, **1986**; d) C. E. Foster, GB2.430.936, **2007**; e) C. Rădulescu, *Rev. Chim.* **2005**, *56*, 151–154; f) C. Rădulescu, A.-M. Hossu, *Rev. Chim.* **2005**, *56*, 742–745; g) J. Fleischhauer, R. Beckert, DE102007050673, **2007**; h) G. J. Richards, J. P. Hill, N. K. Subbaiyan, F. D'Souza, P. A. Karr, M. R. J. Elsegood, S. J. Teat, T. Mori, K. Ariga, *J. Org. Chem.* **2009**, *74*, 8914–8923; i) G. J. Richards, J. P. Hill, K. Okamoto, A. Shundo, M. Akada, M. R. J. Elsegood, T. Mori, K. Ariga, *Langmuir* **2009**, *25*, 8408–8413; j) J. Fleischhauer, R. Beckert, Y. Jüttke, D. Hornig, W. Günther, E. Birckner, U.-W. Grummt, H. Görls, *Chem. Eur. J.* **2009**, *15*, 12799–12806; k) A. R. Ahmad, L. K. Mehta, J. Parrick, *J. Chem. Soc. Perkin Trans I* **1996**, 2443–2449; l) Y. Akimoto, *Bull. Chem. Soc. Jpn.* **1956**, *29*, 460–464; m) Y. Akimoto, *Bull. Chem. Soc. Jpn.* **1956**, *29*, 553–559.
- [6] a) F. Stöckner, C. Käpplinger, R. Beckert, H. Görls, *Synlett* **2005**, 643–645; b) F. Stöckner, R. Beckert, D. Gleich, E. Birckner, W. Günther, H. Görls, G. Vaughan, *Eur. J. Org. Chem.* **2007**, 1237–1243.
- [7] a) I. L. Yudin, A. B. Sheremetev, O. P. Shitov, V. A. Tartakovskii, *Mendeleev Commun.* **1995**, *5*, 196–197; b) C. G. Allison, R. D. Chambers, J. A. H. MacBride, W. K. R. Musgrave, *J. Chem. Soc. C* **1970**, 1023–1029.
- [8] O. Tverskoy, F. Rominger, A. Peters, H.-J. Himmel, U. W. F. Bunz, *Angew. Chem.* **2011**, *123*, 3619–3622; *Angew. Chem. Int. Ed.* **2011**, *50*, 3557–3560.
- [9] Such problems are common when working with  $\pi$ -expanded chromophores that tend to form tightly packed aggregates. In this initial study we did not introduce solubilising or bulky groups to prevent  $\pi$  stacking but work to this end is in progress to achieve highly functionalised and well-soluble oligoazaacene derivatives.
- [10] CCDC 819883 (**3a**), 831397 (**4a**), 819884 (**4HHa**) and 819885 (**9**) contain the supplementary crystallographic data for this paper. These data can be obtained free of charge from The Cambridge Crystallographic Data Centre via [www.ccdc.cam.ac.uk/data\\_request/cif](http://www.ccdc.cam.ac.uk/data_request/cif).
- [11] a) F. Wudl, P. A. Koutentis, A. Weitz, B. Ma, T. Strassner, K. N. Houk, S. I. Khan, *Pure Appl. Chem.* **1999**, *71*, 295–303; b) P. A. Koutentis, *ARKIVOC* **2002**, *VI*, 175–191; c) A. E. Riley, G. W. Mitchell, P. A. Koutentis, M. Bendikov, P. Kaszynski, F. Wudl, S. H. Tolbert, *Adv. Funct. Mater.* **2003**, *13*, 531–540.
- [12] C. Reichardt in *Solvents and Solvent Effects in Organic Chemistry* Wiley-VCH, Weinheim, **2004**, p. 329.
- [13] G. A. Crosby, J. N. Demas, *J. Phys. Chem.* **1971**, *75*, 991–1024.
- [14] S. Daehne, *Chimia* **1991**, *45*, 288–296.
- [15] Gaussian 03, Revision D.01, M. J. Frisch, G. W. Trucks, H. B. Schlegel, G. E. Scuseria, M. A. Robb, J. R. Cheeseman, J. A. Montgomery, Jr., T. Vreven, K. N. Kudin, J. C. Burant, J. M. Millam, S. S. Iyengar, J. Tomasi, V. Barone, B. Mennucci, M. Cossi, G. Scalmani, N. Rega, G. A. Petersson, H. Nakatsuji, M. Hada, M. Ehara, K. Toyota, R. Fukuda, J. Hasegawa, M. Ishida, T. Nakajima, Y. Honda, O. Kitao, H. Nakai, M. Klene, X. Li, J. E. Knox, H. P. Hratchian, J. B. Cross, C. Adamo, J. Jaramillo, R. Gomperts, R. E. Stratmann, O. Yazyev, A. J. Austin, R. Cammi, C. Pomelli, J. W. Ochterski, P. Y. Ayala, K. Morokuma, G. A. Voth, P. Salvador, J. J. Dannenberg, V. G. Zakrzewski, S. Dapprich, A. D. Daniels, M. C. Strain, O. Farkas, D. K. Malick, A. D. Rabuck, K. Raghavachari, J. B. Foresman, J. V. Ortiz, Q. Cui, A. G. Baboul, S. Clifford, J. Cioslowski, B. B. Stefanov, G. Liu, A. Liashenko, P. Piskorz, I. Komaromi, R. L. Martin, D. J. Fox, T. Keith, M. A. Al-Laham, C. Y. Peng, A. Na-

- nayakkara, M. Challacombe, P. M. W. Gill, B. Johnson, W. Chen, M. W. Wong, C. Gonzalez, J. A. Pople, Gaussian, Inc., Wallingford CT, **2004**.
- [16] A. P. Demchenko, Y. Mély, G. Duportail, A. S. Klymchenko, *Biophys. J.* **2009**, *96*, 3461–3470.
- [17] K. Eichkorn, F. Weigend, O. Treutler, R. Ahlrichs, *Theor. Chem. Acc.* **1997**, *97*, 119–124.
- [18] F. L. Hirshfeld, *Theoret. Chim. Acta* **1977**, *44*, 129–138.
- [19] K. B. Wiberg, *Tetrahedron* **1968**, *24*, 1083–1096.
- [20] R. Krishnan, J. S. Binkley, R. Seeger, J. A. Pople, *J. Chem. Phys.* **1980**, *72*, 650–654.
- [21] a) M. J. Allen, D. J. Tozer, *Mol. Phys.* **2002**, *100*, 433–439; b) G. Zhang, C. B. Musgrave, *J. Phys. Chem. A* **2007**, *111*, 1554–1561.

Received: October 25, 2011  
Published online: March 5, 2012